THE JOURNAL OF PHYSICAL CHEMISTRY B

Article

pubs.acs.org/JPCB

Examination of Tyrosine/Adenine Stacking Interactions in Protein Complexes

Kari L. Copeland,[†,¶] Samuel J. Pellock,[‡] James R. Cox,[‡] Mauricio L. Cafiero,[§] and Gregory S. Tschumper*[,†]

[†]Department of Chemistry and Biochemistry, University of Mississippi, University, Mississippi 38677, United States

[‡]Department of Chemistry, Murray State University, Murray, Kentucky 42071, United States

[§]Department of Chemistry, Rhodes College, Memphis, Tennessee 38112, United States

Supporting Information

ABSTRACT: The π-stacking interactions between tyrosine amino acid side chains and adenine-bearing ligands are examined. Crystalline protein structures from the protein data bank (PDB) exhibiting face-to-face tyrosine/adenine arrangements were used to construct 20 unique 4-methylphenol/N9-methyladenine (*p*-cresol/9MeA) model systems. Full geometry optimization of the 20 crystal structures with the M06-2X density functional theory method identified 11 unique low-energy conformations. CCSD(T) complete basis set (CBS) limit interaction energies were estimated for all of the structures to determine the magnitude of the interaction between the two ring systems. CCSD(T) computations with double-ζ basis sets (e.g., 6-31G*(0.25) and aug-cc-pVDZ) indicate that the MP2 method overbinds by as much as 3.07 kcal mol^{-1} for the crystal structures and 3.90 kcal mol^{-1} for the optimized structures. In the 20 crystal structures, the estimated CCSD(T) CBS limit interaction energy ranges from −4.00 to −6.83 kcal mol^{-1}, with an average interaction energy of −5.47 kcal mol^{-1}, values remarkably similar to the corresponding data for phenylalanine/adenine stacking interactions. Geometry optimization significantly increases the interaction energies of the *p*-cresol/9MeA model systems. The average estimated CCSD(T) CBS limit interaction energy of the 11 optimized structures is 3.23 kcal mol^{-1} larger than that for the 20 crystal structures.

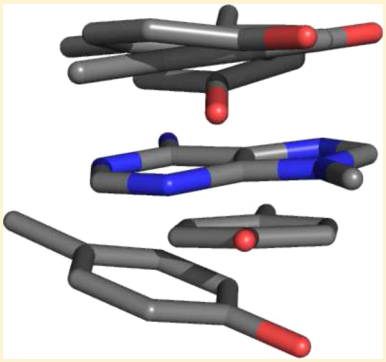

INTRODUCTION

Noncovalent interactions provide a flexible framework for many biological processes to occur. They maintain a relatively weak interaction while, at the same time, affording great stabilizing effects to the system. For instance, these characteristics of noncovalent interactions allow for biomacromolecules to assemble and fold.[1] Flexibility is important, because noncovalent interactions take place in systems that are constantly changing, and it can even facilitate the opening and closing of active sites/pockets.[2−7] In the body, adenosine 5′-triphosphate (ATP) interacts with proteins in its vicinity to carry out functions such as energy transfer, cell signaling, and protein synthesis.[8,9] Drug design often exploits noncovalent interactions and their properties in the development of pharmaceuticals that exhibit protein−drug binding.[10−12]

A particularly interesting subset of noncovalent interactions are those involving aromatic species, and an entire issue of *Accounts of Chemical Research* was recently dedicated to the broad range of chemistry influenced by aromatic interactions.[13] The attractive interactions between aromatic system can be quite substantial even when they are uncharged, and these neutral $\pi\cdots\pi$ interactions play vital roles in the biochemistry of nucleic acids and proteins.[14−27]

The present study extends our previous investigation of aromatic protein/ligand stacking interactions between adenine-bearing ligands and the side chains of phenylalanine[28] to tyrosine amino acid residues. The tyrosine/adenine interaction has been recognized for its role in cellular processes involving protein complexes. For example, the stacking interaction between the aromatic side chain of tyrosine and adenine has also been shown to be involved in the disruption of DNA bases for the purposes of binding RNA polymerase to promoter DNA.[29] The work presented here also complements other efforts to characterize neutral $\pi\cdots\pi$ interactions between aromatic amino acid residues and natural DNA and RNA nucleobases with quantum mechanical electronic structure computations.[17,30−37] Although the chemical environment (e.g., solvent and biopolymer backbones) certainly influences protein−nucleic acid complexation, careful calibration has revealed that the fundamental nature and magnitude of the $\pi\cdots\pi$ interactions is not significantly perturbed as long as the interacting fragments are not charged.[35−37]

Here we probe protein/ligand interactions between tyrosine amino acid side chains and adenine-bearing ligands. Dimer models composed of 4-methylphenol/N9-methyladenine (*p*-cresol/9MeA) were constructed from 20 X-ray crystal

Received: August 11, 2013
Revised: October 4, 2013

   dx.doi.org/10.1021/jp408027j | *J. Phys. Chem. B* XXXX, XXX, XXX−XXX

structures identified in the Protein Data Bank (PDB). Estimates of the CCSD(T) complete basis set (CBS) limit interaction energies are reported for these native crystal structure configurations as well as for their fully optimized (energy minimized) geometries. The energetics of these *p*-cresol/9MeA complexes are compared and contrasted with those of related systems, particularly the toluene/9MeA models of phenylalanine/adenine interactions.

COMPUTATIONAL METHODS

Crystal structures were obtained from the Research Collaboratory for Structural Bioinformatics (RCSB) Protein Data Bank (PDB).[38] The ReliBase program[39] was used to search the data bank for protein−ligand complexes that contained tyrosine/adenine stacking interactions. Protein complexes containing a tyrosine ring ligand were first selected.[40] Next, the search results were refined with the Protein Explorer program[41] to identify complexes with an adenine ring in the vicinity of the tyrosine residue. Finally, tyrosine/adenine complexes were selected for this study when they were no more than 4.5 Å apart and qualitatively adopted a parallel face-to-face orientation. This procedure identified 20 stacking interactions between tyrosine side chains and adenine-bearing ligands in 19 crystal structures whose PDB codes are hereafter used as labels: 1AMO, 1A0I, 1B0U, 1BJK, 1BX0, 1CNF, 1COW, 1CR2, 1CX4, 1D9Z, 1DDG, 1DGS, 1DGY, 1DQA, 1E0J, 1FB3, 1G18, 1MAB, and 1OBT. Note, however, that two contacts were identified in the 1AMO crystal structure. As such, their labels also include the residue number of the tyrosine involved in the stacking interaction ($1AMO_{604}$ and $1AMO_{478}$) to distinguish between them.

Phenol and adenine have been used elsewhere to model the interactions between side chain of tyrosine and DNA/RNA.[31,32,34] Slightly larger models are used here, 4-methylphenol (*p*-cresol) and N9-methyladenine (9MeA). The minimum-energy structures of both are shown in Figure 1.

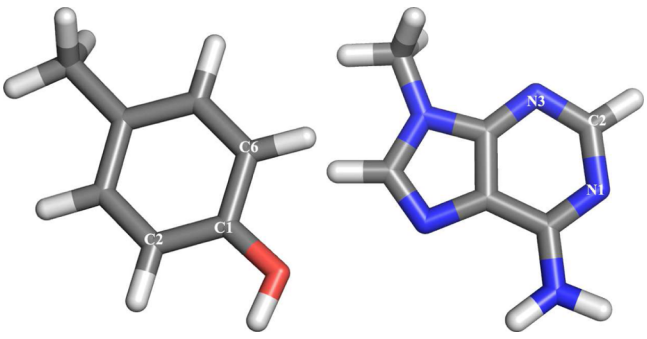

Figure 1. Structures of *p*-cresol (left) and of 9MeA (right) from M06-2X/6-31++G(d,2p) geometry optimizations.

The additional methyl group does not induce noticeable structural changes. For example, *p*-cresol maintains the C_s symmetry of its phenol core. Similarly, the amino group in 9MeA is nearly coplanar with the ring system, just like adenine.[42,43] In both *p*-cresol and 9MeA, only two of the methyl H atoms lie appreciably out of the (pseudo)plane of the ring systems.

The 20 models of tyrosine/adenine-bearing ligand complexes were generated by first removing all atoms not associated with the *p*-cresol and 9MeA fragments. The PDB files do not contain the coordinates of the H atoms because they were not resolved in the X-ray crystal structures. Consequently, hydrogen atoms were added to fill the open valencies giving stacked dimers of *p*-cresol and 9MeA. The initial orientations of the hydrogen atoms mimicked those in the monomers (Figure 1). The positions of the H atoms were then optimized using Merck Molecular Force Field (MMFF)[44] in the Spartan'04 software package[45] while freezing the coordinates of all other atoms. These constrained MMFF optimizations did not substantially change the (nearly) coplanar orientations of the hydroxyl and amino H atoms in the *p*-cresol and 9MeA fragments. The resulting stacked *p*-cresol/9MeA dimers referred to as "crystal structures" in this study and their Cartesian coordinates are provided in the Supporting Information.

Full geometry optimizations were performed on all 20 crystal structures with the M06-2X density functional theory (DFT) method[46] and the 6-31++G(d,2p) basis set. This functional has been shown to provide a good description of both stacked and T-shaped interactions in closely related systems.[47] All DFT computations were performed with the Gaussian 09[48] software package and employed the ultrafine pruned numerical integration grid with 99 radial shells and 590 angular points per shell. Rather tight convergence criteria were adopted for the geometry optimizations. The maximum residual internal force after all DFT optimizations was less than 1.5×10^{-5} hartree/bohr (or hartree/radian).

A second set of optimizations were performed in an attempt to identify additional low-energy configurations of the stacked *p*-cresol/9MeA dimer. In this alternate procedure, the 20 crystal structures were initially optimized with the MMFF in Spartan'04. These structures were then refined with the aforementioned M06-2X/6-31++G(d,2p) optimizations.

Harmonic vibrational frequencies were computed for all 40 structures obtained from the two optimization procedures (DFT-only and MMFF+DFT). The vibrational frequencies were used not only to confirm that each stationary point corresponds to a minimum on the potential energy surface (PES) but also to help compare structures with nearly identical electronic energies. A total of 11 unique "optimized structures" were identified by this process.

Interaction energies (E_{int}) were determined for the crystal structures by subtracting the electronic energies of the noninteracting fragments from the energy of the complex structure.

$$E_{int} = E(p\text{-cresol/9MeA}) - E(p\text{-cresol}) - E(\text{9MeA}) \quad (1)$$

A standard Boys and Bernardi counterpoise (CP) correction[49,50] was applied to address the inconsistency commonly referred to as basis set superposition error (BSSE).[51] As such, the fragment energies in eq 1 were computed in the basis set of the complex.

The analogous procedure was applied to the optimized structures. However, the fragment relaxation/distortion energies must also be computed in the fragment basis set because the structures of *p*-cresol and 9MeA were also optimized at the same level of theory as the complexes. Technically, this quantity is the binding energy, but it will still be referred to as E_{int} for sake of consistency. To provide an unambiguous description of this quantity, a somewhat cumbersome notation is introduced for the fragment calculations, $E_Z^Y(X)$, where X is the fragment examined, Y indicates the basis set (fragment or complex), and Z denotes the geometry (optimized fragment or complex).

dx.doi.org/10.1021/jp408027j | J. Phys. Chem. B XXXX, XXX, XXX−XXX

$$E_{int} = E(p\text{-cresol/9MeA}) - E^{complex}_{complex}(p\text{-cresol}) - E^{complex}_{complex}(9\text{MeA}) + [E^{fragment}_{complex}(p\text{-cresol}) - E^{fragment}_{fragment}(p\text{-cresol})] + [E^{fragment}_{complex}(9\text{MeA}) - E^{fragment}_{fragment}(9\text{MeA})] \quad (2)$$

For the 20 crystal structures, the nuclear configurations of the fragments are frozen/rigid in the complex (i.e., no relaxation of the fragments). In this case, the relaxation/distortion energies in square brackets vanish, and eq 2 reduces to eq 1.

The electronic energies associated with eqs 1 and 2 were computed with size-consistent correlated ab initio methods. MP2 complete basis set (CBS) limit electronic energies, $E^{MP2/CBS}_{int}$, were estimated with explicitly correlated MP2-F12 computations (employing the 3C(FIX) ansatz).[52−55] The corresponding cc-pVDZ-F12 basis set (denoted VDZ-F12) was used.[56,57] It is now widely recognized that a reliable description of π-type noncovalent interactions of this nature requires sophisticated electronic structure methods.[26,58−60] CCSD(T) computations were performed with the 6-31G*(0.25) basis set[61] with α_d = 0.25 for C, N, and O to assess higher order correlation effects. The popular $\delta^{CCSD(T)}_{MP2}$ correction was determined for each structure by taking the difference between CCSD(T) and MP2 interaction energies. CP corrections were not applied in this case, because they have been shown not to have substantial effects on $\delta^{CCSD(T)}_{MP2}$.[62−64]

$$\delta^{CCSD(T)}_{MP2} = \Delta E^{CCSD(T)/6\text{-}31G*(0.25)}_{int} - \Delta E^{MP2/6\text{-}31G*(0.25)}_{int} \quad (3)$$

This correction term was then combined with MP2 CBS limit interaction energies ($E^{MP2/CBS}_{int}$) to estimate the electronic interaction energy at the CCSD(T) CBS limit ($E^{CCSD(T)/CBS}_{int}$) for each structure.

$$E^{CCSD(T)/CBS}_{int} = E^{MP2/CBS}_{int} + \delta^{CCSD(T)}_{MP2} \quad (4)$$

A thorough analysis of the basis set dependence of the $\delta^{CCSD(T)}_{MP2}$ term[64] has revealed that the 6-31G*(0.25) and aug-cc-pVDZ[65,66] basis sets have very similar performance. For simple model systems containing C, H, and N, the mean absolute deviation from the CBS limit $\delta^{CCSD(T)}_{MP2}$ values is 0.11 kcal mol^{-1} for the 6-31G*(0.25) basis set and 0.12 kcal mol^{-1} for the aug-cc-pVDZ basis set, while the maximum deviations were 0.37 and 0.33 kcal mol^{-1}, respectively. As such, we expect the higher-order correlation corrections computed here with the 6-31G*(0.25) basis set to be within a few tenths of a kcal mol^{-1} of the CBS value. Nevertheless, CCSD(T) computations were also performed on a few structures with "heavy"-aug-cc-pVDZ basis set (haDZ) that only places diffuse functions on the heavy (non-hydrogen) atoms (i.e., cc-pVDZ for H and aug-cc-pVDZ for C, N, O).

All MP2 and CCSD(T) energy point computations employed the frozen-core approximation and were performed using the Molpro 2010 software package.[67] The default density fitting and resolution of the identity basis sets were used for the MP2-F12 computations.

RESULTS

Structures. An overlay of the 20 *p*-cresol/9MeA crystal structure models of π-stacking in protein/adenine-bearing ligand complexes is shown in Figure 2. Their Cartesian coordinates are reported in the Supporting Information. Unlike the phenylalanine systems examined in our previous study,[28] the side chain of tyrosine can potentially donate a hydrogen bond to or accept a hydrogen bond from adenylate ligands. Unfortunately, the positions of the hydrogen atoms were not resolved in the crystal structures. The procedures used to determine positions of the H atoms described in the Computational Methods did not produce any direct O—H···N or N—H···O contacts between *p*-cresol and 9MeA in any of these 20 crystal structure configurations. The hydroxyl and amino H atoms essentially remained in the plane of the corresponding ring systems. Consequently, the interactions in these 20 crystal structure models appear to be predominantly of a face-to-face stacking nature and are comparable to the stacked structures reported in other investigations that have employed rigid phenol and adenine monomers.[31,32,34]

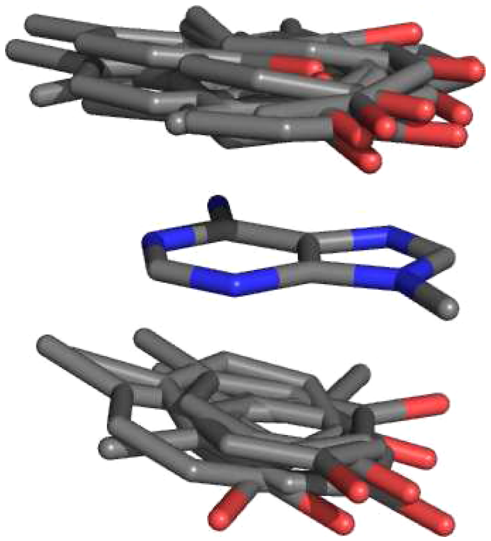

Figure 2. Overlay of the 20 crystal structures for the *p*-cresol/9MeA model complexes. The O atom of *p*-cresol is red and H atoms are not shown.

Full geometry optimizations were performed on each of the crystal structures to partially address the uncertainty associated with the positions of the H atoms. Without any frozen coordinates, the complexes can relax to more strongly interacting configurations, sometimes by forming O—H···N or N—H···O contacts between the *p*-cresol and 9MeA fragments. The optimization procedures described in the previous section identified 11 unique stationary points on the M06-2X/6-31++G(d,2p) PES that are labeled optA, optB, etc. in order of increasing electronic energy at that level of theory. An overlay of these geometrical arrangements is shown in Figure 3. Some optimized structures are very similar and virtually indistinguishable in the overlay. However, even the most similar optimized configurations had certain harmonic vibrational frequencies that differed by at least two dozen wavenumbers, whereas deviations never exceed 1 cm^{-1} for equivalent optimized structures. The Cartesian coordinates of these 11 optimized structures are provided in the Supporting Information for readers interested in a detailed structural analysis.

Harmonic vibrational frequencies indicate that all but one of the optimized structures are minima. Only the optD stationary point has an imaginary vibrational frequency. With a value of only 3*i* cm^{-1}, however, it is feasible that the optD structure is minimum. Additionally, the M06-2X functional does not always correctly predict the Hessian index (number of imaginary vibrational frequencies) for weakly bound systems,[68] and this

dx.doi.org/10.1021/jp408027j | J. Phys. Chem. B XXXX, XXX, XXX−XXX

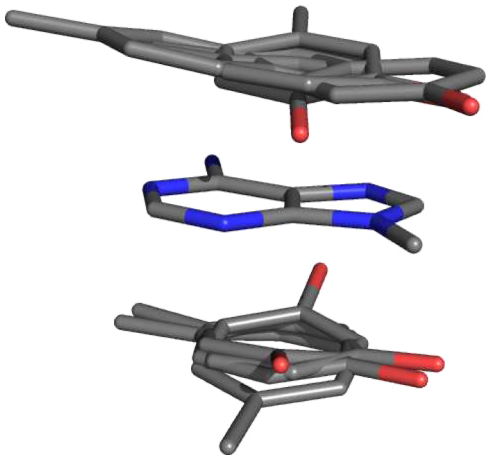

Figure 3. Overlay of the 11 optimized structures for the *p*-cresol/9MeA model complexes. The O atom of *p*-cresol is red and H atoms are not shown.

quantity can also be sensitive to the quality of the numerical integration grid.[69] It should also be noted that both identity and distribution of the optimized structures are dependent upon the details of the optimization procedures. (See Supporting Information for the relationships between the 20 crystal structures and the 11 optimized stationary points.) Changing the method, basis set, or even the optimization algorithm can potentially change the number and distribution of structures identified. It is likely that other low-energy structures exist, but those reported in this work are representative face-to-face configurations of *p*-cresol/9MeA complexes.

The distance, R in Å, between the center of mass of *p*-cresol and the center-of-mass of 9MeA is reported in Tables 1 and 2. The angle, θ in degrees, between the rings of *p*-cresol and 9MeA is also reported in Tables 1 and 2. The plane of the adenine ring is defined by the N1, C2, and N3 atoms (Figure 1). The C1, C2, and C6 atoms (Figure 1) define the plane of the *p*-cresol ring. The 20 crystal structures (shown in Figure 2) all have non-hydrogen atoms in the exact position specified in the PDB crystal structure files of the original protein complexes. The intermolecular distances (R) between the rings range from 4.24 Å (for 1A01) to 3.39 Å (for 1DDG). Full geometry optimizations consistently decreased the distance between the fragment centers-of-mass, sometimes by more than 1 Å. For the fully optimized structures, R ranges from 3.19 to 3.74 Å. Crystal structures have an average R distance of 3.77 Å, while optimized structures have an average R distance of 3.31 Å.

In many cases, geometry optimization also often caused the rings to adopt a more parallel stacking arrangement as indicated by the angle θ between ring planes. The only optimized structures for which θ approaches or exceeds 10° (optA, optB, optC, and optK) are those exhibiting O—H···N and/or N—H···O contacts. They are the only four configurations in which the hydroxyl H atom moves appreciably out of the pseudoplane of the ring system to point toward an N atom in 9MeA. In the case of optD, the amino group H atoms also move out of the pseudoplane of 9MeA, and one is directed toward the O atom in *p*-cresol.

Energetics. Estimates of the MP2 and CCSD(T) CBS limit interaction energies (E_{int}) of the 20 crystal structures are reported in Table 1. At the estimated MP2 CBS limit interaction energies for the crystal structures are between −5.81 kcal mol^{-1} (for 1D9Z) and −9.47 kcal mol^{-1} (for 1B0U). As expected, MP2 overestimates E_{int} in every case for π-stacking (by at least +1.72 kcal mol^{-1}). The $\delta E_{MP2}^{CCSD(T)}$ term accounts for higher order correlation effects, which are quite large (averaging +2.33 kcal mol^{-1}). Combining $\delta E_{MP2}^{CCSD(T)}$ with $E_{int}^{MP2/CBS}$ yields an estimate of the CCSD(T) CBS limit interaction energy ($E_{int}^{CCSD(T)}E$). At the CCSD(T) CBS limit, interaction energies for the crystal structures range from −4.00 kcal mol^{-1} (for 1D9Z) to −6.83 kcal mol^{-1} (for 1COW).

Table 1. Intermolecular Distances (R in Å), Angles (θ in deg), and Estimated CBS Limit Interaction Energies (E_{int} in kcal mol^{-1}) of the 20 Crystal *p*-Cresol/9MeA Structures

structure	R^a	θ^b	$E_{int}^{MP2/CBS}$	$\delta E_{MP2}^{CCSD(T)}$	$E_{int}^{CCSD(T)/CBS}$
$1AMO_{604}$	3.55	6.7	−7.20	+2.64	−4.56
$1AMO_{478}$	3.70	3.2	−7.23	+2.24	−4.99
1A01	4.24	7.4	−6.54	+1.76	−4.78
1B0U	3.50	5.1	−9.47	+3.02	−6.45
1BJK	3.77	7.6	−7.06	+2.07	−5.00
1BX0	3.86	13.5	−8.46	+2.16	−6.30
1CNF	3.98	7.1	−7.21	+1.72	−5.50
1COW	3.85	11.4	−9.03	+2.20	−6.83
1CR2	3.58	14.7	−8.58	+2.69	−5.89
1CX4	3.68	16.8	−8.61	+2.25	−6.36
1D9Z	4.11	18.2	−5.81	+1.81	−4.00
1DDG	3.39	4.7	−8.57	+3.07	−5.50
1DGS	3.99	2.5	−6.64	+2.20	−4.44
1DGY	3.75	10.8	−6.83	+2.31	−4.53
1DQA	3.65	14.0	−7.72	+2.56	−5.16
1E0J	3.98	10.2	−7.38	+1.84	−5.53
1FB3	3.69	19.2	−7.11	+2.46	−4.66
1G18	3.67	1.0	−8.57	+2.41	−6.15
1MAB	3.77	8.3	−8.88	+2.87	−6.00
1OBT	3.73	8.1	−8.96	+2.25	−6.70
max^c	4.24	19.2	−9.47	+3.07	−6.83
min^d	3.39	1.0	−5.81	+1.72	−4.00
avg	3.77	9.5	−7.79	+2.33	−5.47

^{a}Distance between *p*-cresol and 9MeA centers of mass. ^{b}Angle between *p*-cresol and 9MeA ring planes. ^{c}Largest magnitude for E_{int}. ^{d}Smallest magnitude for E_{int}.

Table 2. Intermolecular Distances (R in Å), Angles (θ in deg), and Estimated CBS Limit Interaction Energies (E_{int} in kcal mol^{-1}) of the 11 Optimized *p*-Cresol/9MeA Structures

structure	R^a	θ^b	$E_{int}^{MP2/CBS}$	$\delta E_{MP2}^{CCSD(T)}$	$E_{int}^{CCSD(T)/CBS}$
optA	3.25	10.4	−13.26	+3.63	−9.63
optB	3.23	9.5	−13.34	+3.70	−9.64
optC	3.23	9.7	−13.36	+3.69	−9.67
optD	3.23	11.1	−12.99	+3.64	−9.35
optE	3.20	2.2	−12.70	+3.87	−8.83
optF	3.21	1.9	−12.47	+3.84	−8.63
optG	3.19	2.2	−12.59	+3.90	−8.70
optH	3.21	1.8	−11.91	+3.79	−8.11
optI	3.22	3.1	−11.92	+3.82	−8.10
optJ	3.72	6.5	−10.88	+3.16	−7.72
optK	3.74	8.4	−10.00	+2.63	−7.37
max^c	3.74	11.1	−13.36	+3.90	−9.67
min^d	3.19	1.8	−10.00	+2.63	−7.37
avg	3.31	6.1	−12.31	+3.61	−8.70

^{a}Distance between *p*-cresol and 9MeA centers of mass. ^{b}Angle between *p*-cresol and 9MeA ring planes. ^{c}Largest magnitude for E_{int}. ^{d}Smallest magnitude for E_{int}.

dx.doi.org/10.1021/jp408027j | J. Phys. Chem. B XXXX, XXX, XXX−XXX

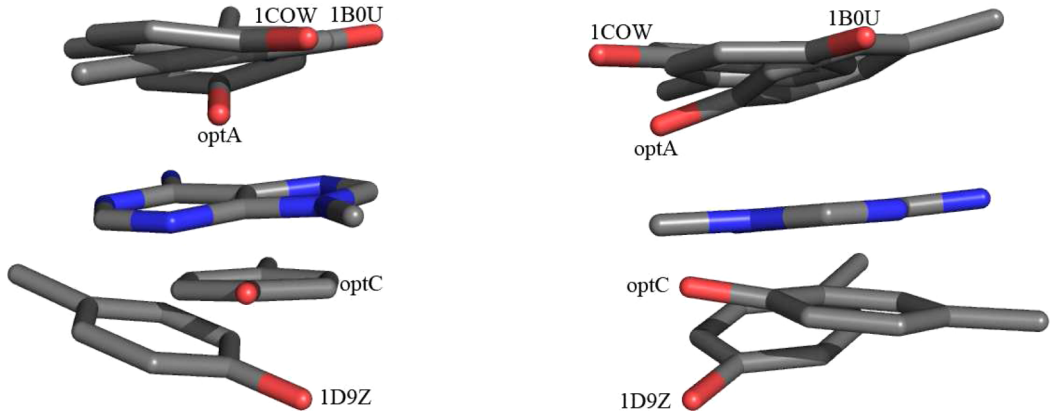

Figure 4. Two perspectives of an overlay depicting the crystal structures with the largest and smallest interaction energies from Table 1 (1D9Z smallest, 1B0U largest MP2/CBS, and 1COW largest CCSD(T)/CBS) along with the two optimized structures with the largest CCSD(T)/CBS interaction energies from Table 2 (optC and optA). The O atom of *p*-cresol is red and H atoms are not shown.

Although the 1COW structure has the largest E_{int} at the estimated CCSD(T) CBS limit, the 1B0U pair bound somewhat more strongly at the estimated MP2 CBS limit (−9.47 versus −9.03 kcal mol^{-1}). The 1D9Z crystal structure has the smallest interaction energy at both the MP2 and the CCSD(T) CBS limits. An overlay of the 1B0U, 1COW, and 1D9Z crystal structures is shown in Figure 4 along with the optA and optC structures. The tendency of the MP2 method to produce a qualitatively different energetic landscape than CCSD(T) highlights the importance of higher order correlation effects when modeling π-type noncovalent interactions in biochemical systems.[27]

Table 2 includes estimates of the MP2 and CCSD(T) CBS limit binding energies of the 11 optimized structures identified at the M06-2X/6-31+G(d,2p) level of theory. Geometry optimization significantly increases the interaction energy of the *p*-cresol/9MeA pairs. The average E_{int} increases by 3.89 kcal mol^{-1} at the estimated MP2 CBS limit and 2.84 kcal mol^{-1} at the CCSD(T) CBS limit as the 20 crystal structures are allowed to relax to the optimized configurations. This increase stems not only from enhanced stacking interactions at optimized geometries but also the formation of O—H···N and N—H···O contacts between *p*-cresol and 9MeA as discussed in the previous section. At the estimated MP2 CBS limit, E_{int} of the 11 unique optimized configurations ranges from −13.36 kcal mol^{-1} (for optC) to −10.00 kcal mol^{-1} (for optK). At the estimated CCSD(T) CBS limit, the optC structure has the largest interaction energy in Table 2 with a value of −9.67 kcal mol^{-1}, just slightly greater than optA and optB (−9.63 and −9.64 kcal mol^{-1}, respectively). It is interesting to note that these three structures (optA, optB, and optC) exhibit an O—H···N contact, but the interaction energies of optE, optF, and optG are only about 1 kcal mol^{-1} smaller even though the hydroxyl and amino H atoms remain in the pseudoplanes of their respective ring systems.

M06-2X/6-31++G(d,2p) interaction energies (with and without CP corrections) are reported in the Supporting Information. Overall, the performance is quite reasonable. The uncorrected M06-2X/6-31++G(d,2p) energies overbind by 1.12−2.12 kcal mol^{-1} (1.82 kcal mol^{-1} on average) relative to the estimated CCSD(T) CBS limit. The average absolute deviation decreases to 0.35 kcal mol^{-1} if a CP correction is performed. Both approaches yield very similar relative energies that deviate from the CCSD(T) CBS values by 0.30 kcal mol^{-1} before a CP correction is applied and 0.24 kcal mol^{-1} after.

Unlike the crystal structures, the MP2 and CCSD(T) methods predict the same qualitative energetic ordering for the optimized structures. However, higher order correlation effects still have a large quantitative effect, as big as +3.90 kcal mol^{-1} for the optG structure and never less than +2.63 kcal mol^{-1}. Note that these $\delta E_{MP2}^{CCSD(T)}$ values are larger for the optimized structures (average = +3.61 kcal mol^{-1}) than the 20 crystal structures for which the largest correction was only +3.07 kcal mol^{-1} and the average was +2.33 kcal mol^{-1}.

The $\delta_{MP2}^{CCSD(T)}$ term was also computed using the haDZ basis set for three structures (1COW, 1D9Z, and optA). The haDZ results do not differ from the 6-31G*(0.25) $\delta_{MP2}^{CCSD(T)}$ values in Tables 1 and 2 by more than 0.14 kcal mol^{-1}. The haDZ data are larger by 0.10 and 0.14 kcal mol^{-1} for 1COW and 1D9Z, respectively, and smaller by 0.11 kcal mol^{-1} for optA.

DISCUSSION

The estimated CCSD(T) CBS limit interaction energies reported for the 20 *p*-cresol/9MeA crystal structures range from −4.00 to −6.83 kcal mol^{-1} with a mean of −5.47 kcal mol^{-1}. These results are remarkably similar to the E_{int} values we reported in an earlier study of 26 toluene/9MeA crystal structure models of phenylalanine/adenine interactions obtained with comparable computational procedures.[28] The average toluene/9MeA E_{int} for those 26 crystal structures was −5.01 kcal mol^{-1} at the estimated CCSD(T) CBS limit, and the maximum was −6.77 kcal mol^{-1} for 1E22 (nearly identical to the −6.83 kcal mol^{-1} reported here for the 1COW crystal structure).

In contrast, the interaction energies of the 11 optimized *p*-cresol/9MeA structures identified in this work are significantly larger than those of the 6 optimized toluene/9MeA configurations reported in Reference 28. Here the estimated CCSD(T) CBS limit interaction energies of the 11 optimized *p*-cresol/9MeA configurations range from −7.37 to −9.67 kcal mol^{-1} with an average of −8.70 kcal mol^{-1}. For the 6 toluene/9MeA optimized structures, E_{int} does not exceed −7.05 kcal mol^{-1} and the average is only −6.54 kcal mol^{-1}.[28] These results are very consistent with other estimates of stacking energies in tyrosine/adenine and phenylalanine/adenine complexes. Estimates of CCSD(T) CBS limit interaction energies from the Wetmore group showed E_{int} of a stacked *p*-cresol/adenine

dx.doi.org/10.1021/jp408027j | J. Phys. Chem. B XXXX, XXX, XXX−XXX

complex is 1.60 kcal mol^{-1} larger than that of a stacked benzene/adenine model when both assume nearly optimal orientations determined from scans of the intermolecular PESs.[32,34]

Our estimates of the CCSD(T) CBS limit energetics indicate that the 20 crystal structure *p*-cresol/9MeA models recover only about half of the optimal stacking energy on average. E_{int} for the crystal structures ranges from 41% to 71% of the −9.67 kcal mol^{-1} interaction energy for the optC structure with an average of 57%. Again, this behavior is different than what was observed in our earlier investigation of 26 toluene/9MeA models of phenylalanine residues interacting with adenine-bearing ligands.[28] In that work, the stacking interactions of toluene/9MeA crystal structures models recovered up to 96% of the maximum interaction energy of an optimized configuration (71% on average).

CONCLUSION

In this study, π-stacking interactions between the aromatic side chain of tyrosine and adenine-bearing ligands were investigated. Crystal structures from the Protein Data Bank (PDB) were used to construct 20 model configurations of 4-methylphenol and N9-methyladenine (*p*-cresol/9MeA). After full geometry optimizations with the M06-2X density functional theory method, the 20 *p*-cresol/9MeA structures collapsed to 11 unique optimized configurations. CCSD(T) CBS limit interaction energies for all of the structures were estimated by combining explicitly correlated MP2-F12 and canonical CCSD(T) computations. As expected for face-to-face π-type interactions of this nature, MP2 significantly overbinds relative to the CCSD(T) method.

At the crystal structure geometries, the interaction energies of the 20 *p*-cresol/9MeA models of tyrosine/adenine interactions examined here are comparable to those of the 26 toluene/9MeA models of phenylalanine/adenine interactions reported earlier[28] (average estimated CCSD(T)/CBS E_{int} values of −5.47 and −5.01 kcal mol^{-1}, respectively). When the geometries of these model complexes are optimized, however, the interaction energies of the *p*-cresol/9MeA systems increase far more than those of the toluene/9MeA structures due to the formation of favorable contacts involving the OH group. At the estimated CCSD(T) CBS limit, the average interaction energy of the 11 optimized *p*-cresol/9MeA configurations is −8.70 kcal mol^{-1} with a maximum of −9.67 kcal mol^{-1} compared to an average E_{int} of −6.54 kcal mol^{-1} and a maximum of −7.05 kcal mol^{-1} for 6 optimized toluene/9MeA structures. Consequently, the toluene/9MeA models recover a far greater percentage of the largest interaction energy associated with their optimized structures (up to 96% and 71% on average) than the *p*-cresol/9MeA systems (up to 71% and 57% on average). These computations indicate that the overall interaction between the side chain of tyrosine and adenine-bearing ligands could be ≈1 kcal mol^{-1} stronger than phenylalanine if it adopts orientations that allow the OH group to establish other contacts (e.g., O−H···N or N−H···O) with the ligand. At the face-to-face orientations adopted in these crystal structures, however, the interaction energies of the tyrosine and phenylalanine models have very similar stacking interaction energies with 9MeA.

We plan to examine other potential O−H···N or N−H···O contacts in a subsequent study that will perform a similar analysis of tyrosine/ligand interactions using larger models of the binding pocket. In particular, we will examine OH and NH_2 orientations that could lead to indirect interactions (via bridging water molecules and neighboring amino acid residues) as well as direct interactions with other parts of the adenylate ligands (e.g., phosphate or sugar moieties). Fortunately, the formation of hydrogen bonds with the OH group of the tyrosine side chain is not expected to significantly perturb the stacking interactions reported here between two neutral fragments, and any additional contributions are anticipated to be largely additive.[35−37]

ASSOCIATED CONTENT

Supporting Information

Cartesian coordinates, interaction energies, and relative energies. This material is available free of charge via the Internet at http://pubs.acs.org.

AUTHOR INFORMATION

Corresponding Author

*E-mail: tschumpr@olemiss.edu.

Present Address

[¶]Jackson State University, Jackson, Mississippi 39217-0510.

Notes

The authors declare no competing financial interest.

ACKNOWLEDGMENTS

The authors thank the Mississippi Center for Supercomputing Research for access to their resources. Financial support for this work was provided in part from the National Science Foundation (CHE-0957317 and EPS-0903787 to G.S.T.), the American Chemical Society-Petroleum Research Fund (39739-B to J.R.C.), the Murray State University Committee on Institutional Studies and Research (101928 to J.R.C.), and the Dr. Jesse D. Jones Endowment for the College of Science, Engineering and Technology at Murray State University (to S.J.P.).

REFERENCES

(1) Fehlner, T. P.; Halet, J.; Saillard, J. *Molecular Cluster: A Bridge to Solid-State Chemistry*; Cambridge University Press: Cambridge, UK, 2007.

(2) Scheraga, H. A., Ed. *Protein Structure*; Academic Press: New York, 1961.

(3) Burley, S. K.; Petsko, G. A. Aromatic-Aromatic Interaction: A Mechanism of Protein Structure Stabilization. *Science* **1985**, *229*, 23−28.

(4) Scheiner, S., Ed. *Molecular Interactions from van der Waals to Strongly Bound Complexes*, 3rd ed.; John Wiley and Sons: Chichester, England, 1997.

(5) McGaughey, G. B.; Gagne, M.; Rappe, A. K. π-Stacking Interaction: Alive and Well in Proteins. *J. Biol. Chem.* **1998**, *273*, 15458−15463.

(6) Whitford, D., Ed. *Proteins: Structure and Function*; John Wiley and Sons: Chichester, England, 2005.

(7) Šponer, J.; Jurecka, P.; Marchan, I.; Luque, F. J.; Orozco, M.; Hobza, P. Nature of Base Stacking: Reference Quantum-Chemical Stacking Energies in Ten Unique B-DNA Base-Pair Steps. *Chem.—Eur. J.* **2006**, *12*, 2854−2865.

(8) Chene, P. ATPases as Drug Targets: Learning from their Structure. *Nat. Rev. Drug Discovery* **2002**, *1*, 665−673.

(9) Mao, L.; Wang, Y.; Liu, Y.; Hu, X. Molecular Determinants for ATP-binding in Proteins: A Data Mining and Quantum Chemical Analysis. *J. Mol. Biol.* **2004**, *336*, 787−807.

(10) Chen, R. J.; Bangaruntip, S.; Drouvalakis, K. A.; Kim, N. W. S.; Shim, M.; Li, Y.; Lim, W.; Utz, P. J.; Dai, H. Noncovalent

Functionalization of Carbon Nanotubes for Highly Specific Electronic Biosensors. *Proc. Natl. Acad. Sci. U.S.A.* **2003**, *100*, 4984−4989.
(11) Copeland, R. A. *Evaluation of Enzyme Inhibitors in Drug Discovery: A Guide for Medicinal Chemists and Pharmacologists*; John Wiley and Sons: Hoboken, NJ, 2005.
(12) Leung, C. S.; Leung, S. S. F.; Tirado-Rives, J.; Jorgensen, W. L. Methyl Effects on Protein-Ligand Binding. *J. Med. Chem.* **2012**, *55*, 4489−4500.
(13) Waters, M. L. Aromatic Interactions. *Acc. Chem. Res.* **2013**, *46*, 873−873.
(14) Baker, C. M.; Grant, G. H. Role of Aromatic Amino Acids in Protein−Nucleic Acid Recognition. *Biopolymers* **2007**, *85*, 456−470.
(15) Černý, J.; Hobza, P. Non-Covalent Interactions in Biomacromolecules. *Phys. Chem. Chem. Phys.* **2007**, *9*, 5281−5388.
(16) Šponer, J.; Riley, K.; Hobza, P. Nature and Magnitude of Aromatic Stacking of Nucleic Acid Bases. *Phys. Chem. Chem. Phys.* **2008**, *10*, 2595−2610.
(17) Cysewski, P. A Post-SCF Complete Basis Set Study on the Recognition Patterns of Uracil and Cytosine by Aromatic and π-Aromatic Stacking Interactions with Amino Acid Residues. *Phys. Chem. Chem. Phys.* **2008**, *10*, 2636−2645.
(18) Improta, R. The Excited States of π-Stacked 9-Methyladenine Oligomers: A TD-DFT Study in Aqueous Solution. *Phys. Chem. Chem. Phys.* **2008**, *10*, 2656−2664.
(19) Cysewski, P.; Czyźnikowska, Ź.; Zaleśny, R.; Czeleń, P. The Post-SCF Quantum Chemistry Characteristics of the Guanine-Guanine Stacking in B-DNA. *Phys. Chem. Chem. Phys.* **2008**, *10*, 2665−2672.
(20) Marsili, S.; Chelli, R.; Schettino, V.; Procacci, P. Thermodynamics of Stacking Interactions in Proteins. *Phys. Chem. Chem. Phys.* **2008**, *10*, 2673−2685.
(21) Morgado, C. A.; Hillier, I. H.; Burton, N. A.; McDouall, J. J. W. A QM/MM Study of Fluoroaromatic Interactions at the Binding Site of Carbonic Anhydrase II, Using a DFT Method Corrected for Dispersive Interactions. *Phys. Chem. Chem. Phys.* **2008**, *10*, 2706−2714.
(22) Lin, I.-C.; Rothlisberger, U. Describing Weak Interactions of Biomolecules with Dispersion-Corrected Density Functional Theory. *Phys. Chem. Chem. Phys.* **2008**, *10*, 2730−2734.
(23) Valdes, H.; Pluháčková, K.; Michal Pitonák, J. Ř.; Hobza, P. Benchmark Database on Isolated Small Peptides Containing an Aromatic Side Chain: Comparison between Wave Function and Density Functional Theory Methods and Empirical Force Field. *Phys. Chem. Chem. Phys.* **2008**, *10*, 2747−2757.
(24) Sharma, R.; McNamara, J. P.; Raju, R. K.; Vincent, M. A.; Hillier, I. H.; Morgado, C. A. The Interaction of Carbohydrates and Amino Acids with Aromatic Systems Studied by Density Functional and Semi-Empirical Molecular Orbital Calculations with Dispersion Corrections. *Phys. Chem. Chem. Phys.* **2008**, *10*, 2767−2774.
(25) Riley, K. E.; Hobza, P. Noncovalent Interactions in Biochemistry. *WIREs Comput. Mol. Sci.* **2011**, *1*, 3−15.
(26) Faver, J. C.; Benson, M. L.; He, X.; Roberts, B. P.; Wang, B.; Marshall, M. S.; Kennedy, M. R.; Sherrill, C. D.; Merz, K. M. Formal Estimation of Errors in Computed Absolute Interaction Energies of Protein−Ligand Complexes. *J. Chem. Theory Comput.* **2011**, *7*, 790−797.
(27) Riley, K. E.; Hobza, P. On the Importance and Origin of Aromatic Interactions in Chemistry and Biodisciplines. *Acc. Chem. Res.* **2013**, *46*, 927−936.
(28) Copeland, K. L.; Anderson, J. A.; Farley, A. R.; Cox, J. R.; Tschumper, G. S. Probing Phenylalanine/Adenine π-Stacking Interactions in Protein Complexes with Explicitly Correlated and CCSD(T) Computations. *J. Phys. Chem. B* **2008**, *112*, 14291−14295.
(29) Schroeder, L. A.; Gries, T. J.; Saecker, R. M.; Record, M. T., Jr.; Harris, M. E.; deHaseth, P. L. Evidence for a Tyrosine−Adenine Stacking Interaction and for a Short-Lived Open Intermediate Subsequent to Initial Binding of Escherichia coli RNA Polymerase to Promoter DNA. *J. Mol. Biol.* **2009**, *385*, 339−349.
(30) Cauët, E.; Rooman, M.; Wintjens, R.; Liévin, J.; Biot, C. Histidine−Aromatic Interactions in Proteins and Protein−Ligand Complexes: Quantum Chemical Study of X-ray and Model Structures. *J. Chem. Theory Comput.* **2005**, *1*, 472−483.
(31) Rutledge, L. R.; Campbell-Verduyn, L. S.; Hunter, K. C.; Wetmore, S. D. Characterization of Nucleobase-Amino Acid Stacking Interactions Utilized by a DNA Repair Enzyme. *J. Phys. Chem. B* **2006**, *110*, 19652−19663.
(32) Rutledge, L. R.; Campbell-Verduyn, L. S.; Wetmore, S. D. Characterization of the Stacking Interactions between DNA or RNA Nucleobases and the Aromatic Amino Acids. *Chem. Phys. Lett.* **2007**, *444*, 167−175.
(33) Ebrahimi, A.; Habibi-Khorassani, M.; Gholipour, A. R.; Masoodi, H. R. Interaction between Uracil Nucleobase and Phenylalanine Amino Acid: the Role of Sodium Cation in Stacking. *Theor. Chem. Acc.* **2009**, *124*, 115−122.
(34) Rutledge, L. R.; Durst, H. F.; Wetmore, S. D. Evidence for Stabilization of DNA/RNA−Protein Complexes Arising from Nucleobase−Amino Acid Stacking and T-Shaped Interactions. *J. Chem. Theory Comput.* **2009**, *5*, 1400−1410.
(35) Churchill, C. D. M.; Rutledge, L. R.; Wetmore, S. D. Effects of the Biological Backbone on Stacking Interactions at DNA-Protein Interfaces: The Interplay between the Backbone$\cdots\pi$ and $\pi\cdots\pi$ Components. *Phys. Chem. Chem. Phys.* **2010**, *12*, 14515−14526.
(36) Rutledge, L. R.; Navarro-Whyte, L.; Peterson, T. L.; Wetmore, S. D. Effects of Extending the Computational Model on DNA−Protein T-shaped Interactions: The Case of Adenine−Histidine Dimers. *J. Phys. Chem. A* **2011**, *115*, 12646−12658.
(37) Leavens, F. M. V.; Churchill, C. D. M.; Wang, S.; Wetmore, S. D. Evaluating How Discrete Water Molecules Affect Protein−DNA π-π and π^+-π Stacking and T-Shaped Interactions: The Case of Histidine-Adenine Dimers. *J. Phys. Chem. B* **2011**, *115*, 10990−11003.
(38) Berman, H. M.; Westbrook, J.; Feng, Z.; Gilliland, G.; Bhat, T. N.; Weissig, H.; Shindyalov, I. N.; Bourne, P. E. The Protein Data Bank. *Nucleic Acids Res.* **2000**, *28*, 235−242; see http://www.rcsb.org (accessed October 1, 2013).
(39) Hendlich, M.; Bergner, A.; Günther, J.; Klebe, G. Relibase: Design and Development of a Database for Comprehensive Analysis of Protein−Ligand Interactions. *J. Mol. Biol.* **2003**, *326*, 607−620; see http://relibase.ccdc.cam.ac.uk (accessed October 1, 2013).
(40) Hendlich, M. Relibase. *Crystallographica D* **1998**, *54*, 1178−1182.
(41) Martz, E. Protein Explorer: Easy Yet Powerful Macromolecular Visualization. *Trends Biochem. Sci.* **2002**, *27*, 107−109; see http://www.umass.edu/microbio/chime/pe_beta/pe/protexpl/frntdoo2.htm (accessed October 1, 2013).
(42) Wang, S.; Schaefer, H. F. The Small Planarization Barriers for the Amino Group in the Nucleic Acid Bases. *J. Chem. Phys.* **2006**, *124*, 044303.
(43) Zierkiewicz, W.; Komorowski, L.; Michalska, D.; Cerny, J.; Hobza, P. The Amino Group in Adenine: MP2 and CCSD(T) Complete Basis Set Limit Calculations of the Planarization Barrier and DFT/B3LYP Study of the Anharmonic Frequencies of Adenine. *J. Phys. Chem. B* **2008**, *112*, 16734−40.
(44) Halgren, T. A. Basis, Form, Scope, Parameterization and Performance of MMFF94. *J. Comput. Chem.* **1996**, *17*, 490−519.
(45) Kong, J.; White, C. A.; Krylov, A. I.; Sherrill, D.; Adamson, R. D.; Furlani, T. R.; Lee, M. S.; Lee, A. M.; Gwaltney, S. R.; Adams, T. R.; et al. Q-Chem 2.0: A High-Performance Ab Initio Electronic Structure Program Package. *J. Comput. Chem.* **2000**, *21*, 1532−1548.
(46) Zhao, Y.; Truhlar, D. The M06 Suite of Density Functionals for Main Group Thermochemistry, Thermochemical Kinetics, Noncovalent Interactions, Excited States, and Transition Elements: Two New Functionals and Systematic Testing of Four M06-Class Functionals and 12 Other Functionals. *Theor. Chem. Acc.* **2008**, *120*, 215−241.
(47) Rutledge, L. R.; Wetmore, S. D. The Assessment of Density Functionals for DNA-Protein Stacked and T-Shaped Complexes. *Can. J. Chem.* **2010**, *88*, 815−830.

(48) Frisch, M. J.; Trucks, G. W.; Schlegel, H. B.; Scuseria, G. E.; Robb, M. A.; Cheeseman, J. R.; Scalmani, G.; Barone, V.; Mennucci, B.; Petersson, G. A. et al. *Gaussian 09, Revision A.1*; Gaussian Inc.: Wallingford CT, 2009; see http://www.gaussian.com (accessed October 1, 2013).
(49) Jansen, H. B.; Ros, P. Non-Empirical Molecular Orbital Calculations on the Protonation of Carbon Monoxide. *Chem. Phys. Lett.* **1969**, *3*, 140−143.
(50) Boys, S. F.; Bernardi, F. The Calculation of Small Molecular Interactions by the Differences of Separate Total Energies. Some Procedures with Reduced Errors. *Mol. Phys.* **1970**, *19*, 553−566.
(51) Liu, B.; Mclean, A. D. Accurate Calculation of the Attractive Interaction of Two Ground State Helium Atoms. *J. Chem. Phys.* **1973**, *59*, 4557−4558.
(52) Kutzelnigg, W. R12-Dependent Terms in the Wave Function as Closed Sums of Partial Wave Amplitudes for Large l. *Theor. Chim. Acta.* **1985**, *68*, 445−469.
(53) Klopper, W.; Kutzelnigg, W. Møller−Plesset Calculations Taking Care of the Correlation CUSP. *Chem. Phys. Lett.* **1987**, *134*, 17−22.
(54) Kutzelnigg, W.; Klopper, W. Wave Functions with Terms Linear in the Interelectronic Coordinates to Take Care of the Correlation Cusp. I. General Theory. *J. Chem. Phys.* **1991**, *94*, 1985−2001.
(55) Klopper, W.; Manby, F. R.; Ten-No, S.; Valeev, E. F. R12 Methods in Explicitly Correlated Molecular Electronic Structure Theory. *Int. Rev. Phys. Chem.* **2006**, *25*, 427−468.
(56) Adler, T. B.; Knizia, G.; Werner, H. A Simple and Efficient CCSD(T)-F12 Approximation. *J. Chem. Phys.* **2007**, *127*, 221106.
(57) Peterson, K. A.; Adler, T. B.; Werner, H. Systematically Convergent Basis Sets for Explicitly Correlated Wavefunctions: The Atoms H, He, B−Ne, and Al−Ar. *J. Chem. Phys.* **2008**, *128*, 084102.
(58) Sherrill, C. D. In *Reviews in Computational Chemistry*; Lipkowitz, K. B., Cundari, T. R., Eds.; Wiley-VCH, Inc.: Hoboken, NJ, 2009; Vol. *26*; pp 1−38.
(59) Tschumper, G. S. In *Reviews in Computational Chemistry*; Lipkowitz, K. B., Cundari, T. R., Eds.; Wiley-VCH, Inc.: Hoboken, NJ, 2009; Vol. *26*, pp 39−90.
(60) Hobza, P. Calculations on Noncovalent Interactions and Databases of Benchmark Interaction Energies. *Acc. Chem. Res.* **2012**, *45*, 663−672.
(61) Hobza, P.; Sponer, J.; Polasek, M. H-Bonded and Stacked DNA Base Pairs: Cytosine Dimer. An Ab Initio Second−Order Møller−Plesset Study. *J. Am. Chem. Soc.* **1995**, *117*, 792−798.
(62) Hopkins, B. W.; Tschumper, G. S. *Ab Initio* Studies of $\pi\cdots\pi$ Interactions: The Effects of Quadruple Excitations. *J. Phys. Chem. A* **2004**, *108*, 2941−2948.
(63) Bates, D. M.; Anderson, J. A.; Oloyede, P.; Tschumper, G. S. Probing the Effects of Heterogeneity on Delocalized $\pi\cdots\pi$ Interaction Energies. *Phys. Chem. Chem. Phys.* **2008**, *10*, 2775−2779.
(64) Carrell, E. J.; Thorne, C. M.; Tschumper, G. S. Basis Set Dependence of Higher-Order Correlation Effects in π-Type Interactions. *J. Chem. Phys.* **2012**, *136*, 014103.
(65) Dunning, T. H. Gaussian Basis Sets for Use in Correlated Molecular Calculations. I. The Atoms Boron through Neon and Hydrogen. *J. Chem. Phys.* **1989**, *90*, 1007.
(66) Kendall, R. A.; Dunning, T. H.; Harrison, R. J. Electron Affinities of the First-Row Atoms Revisited. Systematic Basis Sets and Wave Functions. *J. Chem. Phys.* **1992**, *96*, 6796−6806.
(67) Werner, H.-J.; Knowles, P. J.; Manby, F. R.; Schütz, M.; Celani, P.; Knizia, G.; Korona, T.; Lindh, R.; Mitrushenkov, A.; Rauhut, G. et al. *MOLPRO, version 2010.1, A Package of Ab Initio Programs*, 2010; see http://www.molpro.net (accessed October 1, 2013).
(68) Copeland, K. L.; Tschumper, G. S. Hydrocarbon/Water Interactions: Encouraging Energetics and Structures from DFT but Disconcerting Discrepancies for Hessian Indices. *J. Chem. Theory Comput.* **2012**, *8*, 1646−1656.
(69) Malagoli, M.; Baker, J. The Effect of Grid Quality and Weight Derivatives in Density Functional Calculations of Harmonic Vibrational Frequencies. *J. Chem. Phys.* **2003**, *119*, 12763−12768.